

NOON-state formation from Fock-state Bose-Einstein condensates

H. Cable^a, F. Laloë^b, and W. J. Mullin^c

^a*Centre for Quantum Technologies, National University of Singapore, Singapore 117543*

^b*Laboratoire Kastler Brossel, ENS, UPMC,*

CNRS ; 24 rue Lhomond, 75005 Paris, France

^c*Department of Physics, University of Massachusetts, Amherst, Massachusetts 01003 USA*

NOON states (states of the form $|N\rangle_a |0\rangle_b + |0\rangle_a |N\rangle_b$ where a and b are single particle states) have been used for predicting violations of local realism (Greenberger-Horne-Zeilinger violations) and are valuable in metrology for precision measurements of phase at the Heisenberg limit. We show theoretically how the use of two Fock state Bose-Einstein condensates as sources in a modified Mach-Zehnder interferometer can lead to the creation of the NOON state in which a and b refer to arms of the interferometer and N is a subset of the total number of particles in the two condensates. The modification of the interferometer involves making “side” measurements of a few particles near the sources. These measurements put the remaining particles in a superposition of two phase states, which are converted into NOON states by a beam splitter if the phase states are orthogonal. When they are not orthogonal, a “feedforward” correction circuit is shown to convert them into proper form so a NOON results. We apply the NOON to the measurement of phase. Here the NOON experiment is equivalent to one in which a large molecule passes through two slits. The NOON components can be recombined in a final beam splitter to show interference.

I. INTRODUCTION

NOON states are interesting and useful [1]; they are “all-or-nothing” states, having the form

$$|\Phi\rangle = \frac{1}{\sqrt{2}} [|N\rangle_a |0\rangle_b + |0\rangle_a |N\rangle_b] \quad (1)$$

where the subscripts a and b represent single particle states. Eq. (1) represents a superposition of all N particles in state a and none in b , or none in b and all in a . Such states can have several important applications: 1) Since they are “Schrödinger cat” states of a system with N particles, one might use them to demonstrate the quantum interference of macroscopically distinct objects [2]. 2) They can be used to study violations of quantum realism in the GHZ contradictions [3–5]. 3) They can be used to violate the standard quantum limit and attain the Heisenberg limit in metrology by providing extremely accurate measurements of phase [6]. 4) They have been proposed for use in quantum lithography [7]. NOON states have been made experimentally with N up to ten particles [8–12]. A two-body NOON state can be constructed by allowing two bosons to impinge on either side of a 50-50 beam splitter. This is because the final state will be a superposition of two-particles on either side of the splitter according to the Hong–Ou–Mandel effect [13]. We have shown previously how one can use two Bose-Einstein condensate Fock states as sources for an interferometer that can produce NOON states, with a and b two arms of the interferometer [14, 15].

The essential idea of the interferometer is as follows. By drawing off a portion of our condensate particles into a pair of detectors D1 and D2, we measure phase, which puts the uncounted particles in a double phase state—a Schrödinger cat. If the phase difference of the two cat branches is π , then passing the remaining particles through a beam splitter results in a NOON state in the two output arms of the interferometer. However, this result occurs only if the number of particles initially detected is ideal (equal numbers in D1 and D2). The phase difference can then be adjusted by use of a correction circuit, in which a “feedforward” method sets the transmission coefficient of a side detector D9 to an appropriate value [14]. The result is that a very good approximation to a pure NOON state can almost always be generated whatever the count of the initial detections at D1 and D2.

We begin in Sec. II by introducing the two-stage interferometer, with several parameters to be determined. In Sec. III, we look first at the case that D1 and D2 register the same particle number, and show how a NOON state is obtained at the output by considering the distribution for the relative phase arising from the initial measurement. In Sec. IV, we progress to the general case, for which D1 and D2 detect different particle numbers. To obtain a NOON state at the output, a condition is derived relating the transmission coefficient for D9, and the outcomes at D1, D2 and D9. To address the probabilistic nature of the side detections, the average value for D9 is computed in Sec. V, providing a simple value for the transmission coefficient. In Sec. VI, the scheme is evaluated by applying two NOON quality factors to

the states at the output. The efficiencies of the scheme without and with the correction circuit, taking into account all possible measurement outcomes, are compared and explained in Sec. VIII. Finally, applications of the scheme to phase estimation and to demonstrating quantum interference are given in Sec. VII.

II. INTERFEROMETER

The interferometer to be used is shown in Fig. 1. Two Fock state sources of number N_α and N_β enter the interferometer. We will see that the side detectors 1 and 2, situated immediately after the sources, are a key element; by measuring m_1 and m_2 particles in these detectors, the uncounted particles, in arms 3 and 4, are put into phase states. If the phase relation is correct (equal numbers m_1 and m_2 in detectors D1 and D2) then, when these remaining particles pass through the middle beam splitter, the result (for suitable value of ξ) is a NOON state in arms 5 and 6. However, if $m_1 \neq m_2$ then we will show that the transmission coefficient at detector D9 can be adjusted to a value that corrects the relative phase giving a NOON after the beam splitter at 7-8.

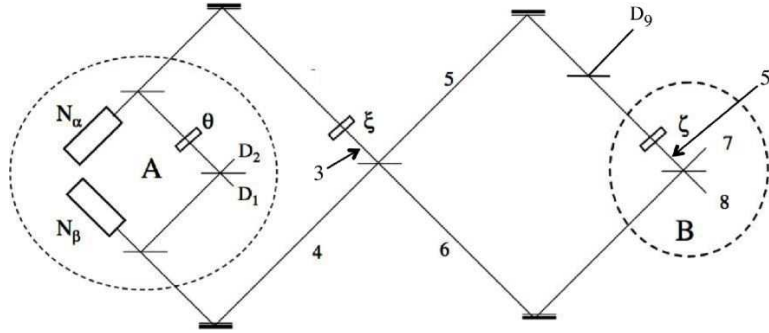


FIG. 1: An interferometer, in which sources have numbers N_α and N_β , which are partially diverted to interfere at a beam splitter and detectors D1 and D2. The counts in these detectors are used to determine the transmission coefficient in the beam splitter leading to D9 correcting the phases of the beams in arms 5' and 6 so that an approximate NOON state emerges 7 and 8. Three phase shifters θ , ξ , and ζ must be properly adjusted.

The annihilation operators at the detectors are found by tracing back from from a detector to each source. We have

$$\begin{aligned}
 a_1 &= \frac{1}{2} (ie^{i\theta} a_\alpha - a_\beta) & a_2 &= \frac{1}{2} (-e^{i\theta} a_\alpha + ia_\beta) \\
 a_5 &= \frac{i}{2} (ie^{i\xi} a_\alpha + a_\beta) & a_{5'} &= \frac{-\sqrt{T}}{2} e^{i\zeta} (ie^{i\xi} a_\alpha + a_\beta) \\
 a_6 &= \frac{1}{2} (ie^{i\xi} a_\alpha - a_\beta) & a_7 &= \frac{1}{2\sqrt{2}} (ue^{i\xi} a_\alpha + va_\beta) \\
 a_8 &= \frac{1}{2\sqrt{2}} (ve^{i\xi} a_\alpha - ua_\beta) & a_9 &= \frac{-i\sqrt{R}}{2} (ie^{i\xi} a_\alpha + a_\beta)
 \end{aligned} \tag{2}$$

where

$$\begin{aligned}
 u &= (\sqrt{T}e^{i\zeta} - 1) \\
 v &= -i(\sqrt{T}e^{i\zeta} + 1)
 \end{aligned} \tag{3}$$

and T and $R = 1 - T$ are the transmission and reflection coefficients at the beam splitter leading to D9. We will immediately take $\theta = \pi/2$, which puts the phase states symmetrically around the zero angle as we will see.

III. CASE WITH NO CORRECTION CIRCUIT

We first look at the uncorrected situation where we select only cases in which $m_1 = m_2$. We then want to show how a NOON state arises in arms 5 and 6. The amplitude for finding particle numbers $\{m_1, m_2, m_5, m_6\}$ in those detectors is

$$C_{m_1, m_2, m_5, m_6} = \left\langle 0 \left| \frac{a_5^{m_5} a_6^{m_6} a_1^{m_1} a_2^{m_2}}{\sqrt{m_1! m_2! m_5! m_6!}} \right| N_\alpha N_\beta \right\rangle \quad (4)$$

Put in the forms from Eq. (2) and expand the binomials to give

$$\begin{aligned} C_{m_1, m_2, m_5, m_6} &\sim \sum_{\{p_i\}} \binom{m_1}{p_1} \binom{m_2}{p_2} \binom{m_5}{p_5} \binom{m_6}{p_6} (-1)^{m_2 - p_2} (ie^{i\xi})^{p_5 + p_6} (-1)^{m_6 - p_6} \\ &\times \left\langle 0 \left| a_\alpha^{p_1 + p_2 + p_5 + p_6} a_\beta^{m_1 + m_2 + m_5 + m_6 - p_1 - p_2 - p_5 - p_6} \right| N_\alpha N_\beta \right\rangle \end{aligned} \quad (5)$$

The second line is evaluated to $\sqrt{N_\alpha! N_\beta!} \delta_{p_1 + p_2 + p_5 + p_6, N_\alpha} \delta_{m_1 + m_2 + m_5 + m_6 - N_\alpha, N}$, where $N = N_\alpha + N_\beta$. For accurate analysis we could replace one of the summation variables by use of the δ -function. But for physical analysis we replace the first by

$$\delta_{p_1 + p_2 + p_5 + p_6, N_\alpha} = \int_{-\pi}^{\pi} \frac{d\phi}{2\pi} e^{i(p_1 + p_2 + p_5 + p_6 - N_\alpha)\phi} \quad (6)$$

Putting this into Eq. (5) we find that each a_α has been replaced by $e^{i\phi}$ and each a_β by 1. The result of redoing the sum is then

$$C_{m_1, m_2, m_5, m_6} = \frac{\sqrt{N_\alpha! N_\beta!}}{2^N \sqrt{m_1! m_2! m_5! m_6!}} \int_{-\pi}^{\pi} \frac{d\phi}{2\pi} e^{-iN_\alpha \phi} R_{12}(\phi) (ie^{i\xi} e^{i\phi} + 1)^{m_5} (ie^{i\xi} e^{i\phi} - 1)^{m_6} \quad (7)$$

where

$$R_{12}(\phi) = (e^{i\phi} + 1)^{m_1} (e^{i\phi} - 1)^{m_2} \quad (8)$$

Factor out $e^{i\phi/2}$, to give

$$R_{12}(\phi) = i^{m_2} 2^M e^{iM\phi/2} Q_{12}(\phi) \quad (9)$$

where $M = m_1 + m_2$ and

$$Q_{12}(\phi) = \left(\cos \frac{\phi}{2} \right)^{m_1} \left(\sin \frac{\phi}{2} \right)^{m_2} \quad (10)$$

For arbitrary m_1, m_2 , the function Q_{12} has peaks at $\pm\phi_0 = \pm 2 \arctan(\sqrt{m_2/m_1})$. In the case $m_1 = m_2$ the plot of Q_{12} has peaks at $\pm\pi/2$ as shown in Fig. 2.

To test for the presence of the NOON state we approximate the peaks in Q_{12} of Fig. 2 by δ -functions:

$$Q_{12}(\phi) \sim \delta(\phi - \phi_0) + (-1)^{m_2} \delta(\phi + \phi_0) \quad (11)$$

The result is then

$$\begin{aligned} C_{m_1, m_2, m_5, m_6} &\sim e^{-iN_\alpha \phi_0} (ie^{i\xi} e^{i\phi_0} + 1)^{m_5} (ie^{i\xi} e^{i\phi_0} - 1)^{m_6} \\ &+ (-1)^{m_2} e^{iN_\alpha \phi_0} (ie^{i\xi} e^{-i\phi_0} + 1)^{m_5} (ie^{i\xi} e^{-i\phi_0} - 1)^{m_6} \end{aligned} \quad (12)$$

When we take $\xi = 0$ and $\phi_0 = \pi/2$ first line is proportional to $0^{m_5} (-2)^{m_6}$ requiring $m_5 = 0$ and $m_6 = N - M$ for non-zero contribution. The second line is proportional to $2^{m_5} 0^{m_6}$ requiring $m_6 = 0$. Thus we get a NOON state with a superposition of $|m_1 m_2 m_5 m_6\rangle = |M/2, M/2, 0, N - M\rangle$ and $|m_1 m_2 m_5 m_6\rangle = |M/2, M/2, N - M, 0\rangle$. To make $\phi_0 = \pi/2$ we must have $m_1 = m_2$.

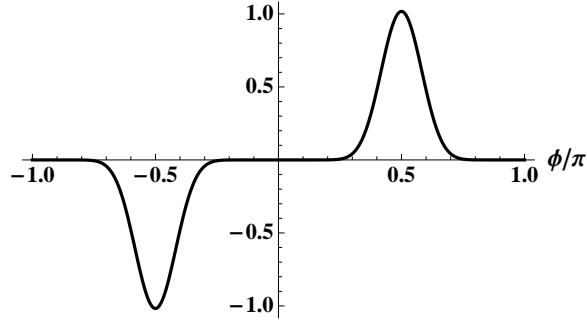


FIG. 2: Plot of $Q_{12}(\phi)$ of Eq. (10) for $m_1 = m_2 = 15$. Because we have taken $\theta = \pi/2$ and $m_1 = m_2$ we find the two peaks at $\pm\pi/2$. For odd m_2 we have one positive and one negative peak. With m_2 even both peaks are positive.

To avoid a numerical integral, we use the δ -function generated in Eq. (5) to keep the probability in the form of a sum:

$$P_{m_1, m_2 m_5, m_6} = K m_5! m_6! \left| \sum_{p, q, r} \frac{e^{-i(p+q)(\xi+\pi/2)} (-1)^{p+r}}{p!(m_1-p)!q!(m_2-q)!r!(m_5-r)!} \right. \\ \left. \times \frac{1}{(N_\alpha - p - q - r)!(p + q + r + m_6 - N_\alpha)!} \right|^2 \quad (13)$$

By adjusting the phase to $\xi = 0$ we get the approximate NOON state as seen in Fig. 3. The NOON state is not perfect because of the finite width of the peaks in Q_{12} . As m_1 and m_2 increase the peaks narrow; in the limit in which they can be replaced by δ -functions, the output state becomes an ideal NOON.

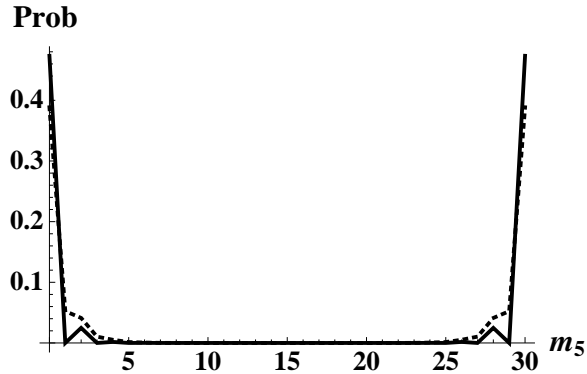


FIG. 3: Plot of $P_{m_1, m_2 m_5, m_6}$ of Eq. (13) versus m_5 ($m_6 = 60 - m_5$) for $N_\alpha = N_\beta = 30$, $m_1 = m_2 = 15$, $\xi = 0$ (solid line). We also show $m_1 = 18$, $m_2 = 12$ (dotted line) to illustrate a case where the phase states are not quite orthogonal. Discrete points are connected by lines as a guide to the eye.

Thus we see in this case that we need m_1 to be only approximately equal to m_2 to get a good approximate NOON state.

IV. THE CORRECTION CIRCUIT

Consider now the complete circuit of Fig. 1. What do we have to do to produce a NOON state in D7 and D8 in the case when $m_1 \neq m_2$? The basic idea to answer this question was given in Ref. 14. The

amplitude for finding the detector counts $\{m_1, m_2, m_7, m_8, m_9\}$ is

$$\begin{aligned}
C_{m_1, m_2, m_7, m_8, m_9} &= \left\langle 0 \left| \frac{a_7^{m_7} a_8^{m_8} a_9^{m_9} a_1^{m_1} a_2^{m_2}}{\sqrt{m_1! m_2! m_7! m_8! m_9!}} \right| N_\alpha N_\beta \right\rangle \\
&\sim \sum_{\{p_i\}} \binom{m_1}{p_1} \binom{m_2}{p_2} \binom{m_7}{p_7} \binom{m_8}{p_8} \binom{m_9}{p_9} (-1)^{m_2 - p_2 + m_8 - p_8} \\
&\quad \times (ie^{i\xi})^{p_9} (e^{i\xi})^{p_7 + p_8} u^{m_8 + p_7 - p_8} v^{m_7 - p_7 + p_8} \\
&\quad \times \delta_{p_1 + p_2 + p_7 + p_8 + p_9, N_\alpha} \delta_{m_1 + m_2 + m_7 + m_8 + m_9, N}
\end{aligned} \tag{14}$$

Replacing the δ -function by an integral as above gives us

$$\begin{aligned}
C_{m_1, m_2, m_7, m_8, m_9} &= \frac{e^{i\eta} \sqrt{R^{m_9}} \sqrt{N_\alpha! N_\beta!}}{2^N \sqrt{2}^{m_7 + m_8} \sqrt{m_1! m_2! m_7! m_8! m_9!}} \int_{-\pi}^{\pi} \frac{d\phi}{2\pi} e^{-iN_\alpha \phi} R_{129}(\phi) \\
&\quad \times (ue^{i\xi} e^{i\phi} + v)^{m_7} (ve^{i\xi} e^{i\phi} - u)^{m_8}
\end{aligned} \tag{15}$$

where η is an unimportant phase and

$$R_{129}(\phi) = (e^{i\phi} + 1)^{m_1} (e^{i\phi} - 1)^{m_2} (ie^{i\xi} e^{i\phi} + 1)^{m_9} \tag{16}$$

We see immediately that if we take $ie^{i\xi} = 1$ then the 9-term has the same binary form as the 1-term and m_1 and m_9 will simply add. With $\xi = -\pi/2$ we have

$$R_{129} = 2^{m_1 + m_2 + m_9} i^{m_2} e^{i(m_1 + m_2 + m_9)\frac{\phi}{2}} \left(\cos \frac{\phi}{2} \right)^{m_1 + m_9} \left(\sin \frac{\phi}{2} \right)^{m_2} \tag{17}$$

which has peaks at $\pm\phi_0 = \pm 2 \arctan(\sqrt{m_2/(m_1 + m_9)})$.

However, for arbitrary ϕ the second line of Eq. (15) becomes (for $e^{i\xi} = -i$),

$$\begin{aligned}
(-iue^{i\phi} + v)^{m_7} (ive^{i\phi} + u)^{m_8} &= (-i)^{m_7} \left[\sqrt{T} e^{i\zeta} (e^{i\phi} + 1) - (e^{i\phi} - 1) \right]^{m_7} \left[\sqrt{T} e^{i\zeta} (e^{i\phi} + 1) + (e^{i\phi} - 1) \right]^{m_8} \\
&= (-i)^{m_7} e^{i(m_7 + m_8)\phi/2} 2^{m_7 + m_8} \left[\sqrt{T} e^{i\zeta} \cos \frac{\phi}{2} - i \sin \frac{\phi}{2} \right]^{m_7} \\
&\quad \times \left[\sqrt{T} e^{i\zeta} \cos \frac{\phi}{2} + i \sin \frac{\phi}{2} \right]^{m_8}
\end{aligned} \tag{18}$$

We can make the factors real if we take $\zeta = \pi/2$, which gives

$$C_{m_1, m_2, m_7, m_8, m_9} = \frac{e^{i\eta} \sqrt{R^{m_9}} \sqrt{N_\alpha! N_\beta!}}{\sqrt{2}^{m_7 + m_8} \sqrt{m_1! m_2! m_7! m_8! m_9!}} \int_{-\pi}^{\pi} \frac{d\phi}{2\pi} e^{i(N_\beta - N_\alpha)\phi/2} Q_{129}(\phi) Q_8(\phi) \left[\sqrt{T} \cos \frac{\phi}{2} - \sin \frac{\phi}{2} \right]^{m_7} \tag{19}$$

where $\mathcal{M} = m_1 + m_2 + m_9$, and

$$Q_{129}(\phi) = \left(\cos \frac{\phi}{2} \right)^{m_1 + m_9} \left(\sin \frac{\phi}{2} \right)^{m_2} \tag{20}$$

$$Q_8(\phi) = \left[\sqrt{T} \cos \frac{\phi}{2} + \sin \frac{\phi}{2} \right]^{m_8} \tag{21}$$

Q_{129} peaks sharply at two angles analogous to Q_{12} of Eq. (10) and, for large m_8 , Q_8 peaks sharply at a different angle; the product also peaks sharply at an intermediate angle. The product $Q_{129}Q_8$ is plotted in Fig. 4 for some specific parameter values to show this.

If m_7 is small, we can assume the last m_7 factor in Eq. (18) (call it $\Delta(\phi)^{m_7}$) is slowly varying compared to the other factor, which can be approximately represented as a δ -function at its maximum angle ϕ_m . Our result for the probability will then have a factor $\Delta(\phi_m)^{m_7}$. If we make $\Delta(\phi_m)$ as small as possible, then the probability will be small for all m_7 except for $m_7 = 0$; that will give us a NOON state.

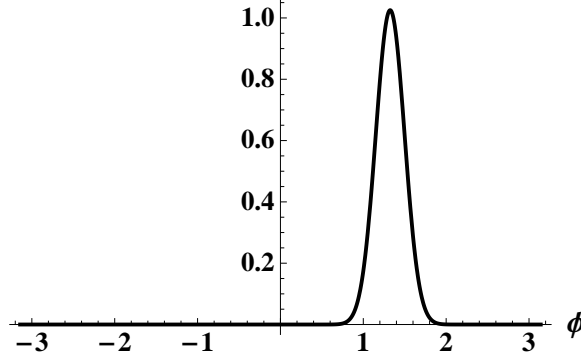


FIG. 4: Plot of $Q_{129}Q_8$ versus ϕ showing that it peaks sharply. The location of the peak is given by the cubic equation given in Eq. (22). Here $m_1 = 22$, $m_2 = 8$, $m_9 = 14$.

We can find the maximum angle of $Q_{129}Q_8$ by taking the logarithmic derivative of the quantity. We take m_{78} equal to the total number of particles entering D7 and D8, that is $m_{78} \equiv m_7 + m_8 = N - m_1 - m_2$. The result of this is the following cubic equation in $X = \tan \frac{\phi_m}{2}$:

$$(m_1 + m_9)X^3 + \sqrt{T}(m_1 + m_9 + m_{78})X^2 - (m_2 + m_{78})X - m_2\sqrt{T} = 0 \quad (22)$$

Also we want $\Delta(\phi_m) = 0$ or

$$\sqrt{T} = X \quad (23)$$

Combining the last two equations gives us a value for T :

$$T = \frac{2m_2 + m_{78}}{2(m_1 + m_9) + m_{78}} \quad (24)$$

Since $m_{78} = N - m_1 - m_2 - m_9$ we have

$$T = \frac{N - (m_1 - m_2 + m_9)}{N + (m_1 - m_2 + m_9)} \quad (25)$$

If $m_1 > m_2$ this value of T will be surely less than one. However, if $m_2 > m_1$ then we will have to go back to Eq. (16) and take $\xi = +\pi/2$ to give an appropriate T value, which has m_1 and m_2 interchanged.

Unfortunately, our value of T depends on the value of m_9 , whose probability distribution in turn depends on T . We consider how to solve this problem in the next section.

V. FINDING m_9

Our expression for T contains m_9 , which we should approximate in some way to get the best NOON state. We want to set the transmission coefficient to a value that depends on the count that just occurred in D1 and D2; of course, then the number going into D9 is probabilistic and is not precisely known. However we could hope to do well enough by replacing m_9 in Eq. (25) by $\langle m_9 \rangle$ so

$$T = \frac{N - (m_1 - m_2 + \langle m_9 \rangle)}{N + (m_1 - m_2 + \langle m_9 \rangle)} \quad (26)$$

We then need to find (for fixed m_1 and m_2) $\langle m_9 \rangle$, which itself depends on T .

We proceed just as before to now look at the probability of finding $m_{5'}, m_6, m_9$ particles just before the last beam splitter in Fig. 1, with given input values of m_1 and m_2 . The amplitude for this is

$$C_{m_1, m_2, m_{5'}, m_6, m_9} = \left\langle 0 \left| \frac{a_1^{m_1} a_2^{m_2} a_{5'}^{m_{5'}} a_6^{m_6} a_9^{m_9}}{\sqrt{m_1! m_2! m_{5'}! m_6! m_9!}} \right| N_\alpha N_\beta \right\rangle \quad (27)$$

We now note that, with the phases chosen, *all* of the operators are of the form $(a_\alpha \pm a_\beta)$ and for $m_1 > m_2$ we have

$$C_{m_1, m_2, m_{5'}, m_6, m_9} = \frac{\sqrt{T^{m_5} R^{m_9}}}{2^N} \left\langle 0 \left| \frac{(a_\alpha + a_\beta)^{m_1 + m_{5'} + m_9} (a_\alpha - a_\beta)^{m_2 + m_6}}{\sqrt{m_1! m_2! m_{5'}! m_6! m_9!}} \right| N_\alpha N_\beta \right\rangle \quad (28)$$

Using this relation we are able to show the following rigorous relation for the average of m_9 over a series of measurements at fixed m_1 and m_2 :

$$\langle m_9 \rangle = (1 - T) (N - m_1 - m_2 - \langle m_6 \rangle) \quad (29)$$

Particle conservation requires

$$\langle m_5 \rangle + \langle m_6 \rangle = N - m_1 - m_2 \quad (30)$$

Further we can prove that an extremely good approximation is given by

$$\langle m_5 \rangle \approx \frac{m_1}{m_2} \langle m_6 \rangle \quad (31)$$

We derive these equations in Appendix A. The physically relevant solutions to these equations, valid for $m_1 \geq m_2$ are

$$T = \frac{m_2}{m_1} \quad (32)$$

$$\langle m_9 \rangle = \frac{m_1 - m_2}{m_1 + m_2} (N - m_1 - m_2) \quad (33)$$

We can actually compute a rigorous numerical average for $\langle m_9 \rangle$ (Appendix B) to show that this formula is quite accurate.

VI. THE CORRECTED NOON STATE

Now let us return to the expression for the NOON probability and compute the distribution with the most probable value of m_9 now known. One possible formula uses the δ -function in Eq. (14) to eliminate p_1 and to find the following result for the probability:

$$P_{m_1, m_2, m_7, m_8, m_9} = \frac{R^{m_9} (m_1 + m_9)!^2 m_7! m_8! N_\alpha! N_\beta!}{4^N 2^{m_7 + m_8} m_1! m_9!} \left| \sum_{p_2 \dots p_8} \frac{(-1)^{p_2}}{(N_\alpha - p_2 - p_7 - p_8)!} \right. \\ \left. \times \frac{(i\sqrt{T} - 1)^{m_8 + p_7 - p_8} (i\sqrt{T} + 1)^{m_7 - p_7 + p_8}}{(m_1 + m_9 + p_2 + p_7 + p_8 - N_\alpha)! p_2! (m_2 - p_2)! p_7! (m_7 - p_7)! p_8! (m_8 - p_8)!} \right|^2 \quad (34)$$

This formula is very general, but has many sums. Nevertheless we can use the angular expression given in Eq. (19), which is also exact and leads to fast and accurate numerical calculations. We have then the alternative formula

$$P_{m_1, m_2, m_7, m_8, m_9} = \frac{R^{m_9} N_\alpha! N_\beta!}{2^{m_7 + m_8} m_1! m_2! m_7! m_8!} \left| \int_{-\pi}^{\pi} \frac{d\phi}{2\pi} e^{-i(N_\alpha - N_\beta)\phi/2} \left(\cos \frac{\phi}{2} \right)^{m_1 + m_9} \left(\sin \frac{\phi}{2} \right)^{m_2} \right. \\ \left. \times \left[\sqrt{T} \cos \frac{\phi}{2} + \sin \frac{\phi}{2} \right]^{m_8} \left[\sqrt{T} \cos \frac{\phi}{2} - \sin \frac{\phi}{2} \right]^{m_7} \right|^2 \quad (35)$$

This probability is symmetric in exchange of m_7 and m_8 ; to see this, after the interchange, simply set $\phi = -\phi$ and the result is the same. We summarize the procedure: For a given m_1, m_2 we determine T and $\langle m_9 \rangle$ from Eqs. (32) and (33). The value of m_9 used in the probability (other than in the T and R values themselves) should be at or near the most probable value (rounded to the nearest integer) since the probability distribution is fairly narrow (see Appendix B).

In the first trial we pick the most probable m_9 value and then a less probable value of m_9 with use of the optimum T value. In the case shown in Fig. 5 e, $N_\alpha = N_\beta = 35, m_1 = 22, m_2 = 8$, the value of the

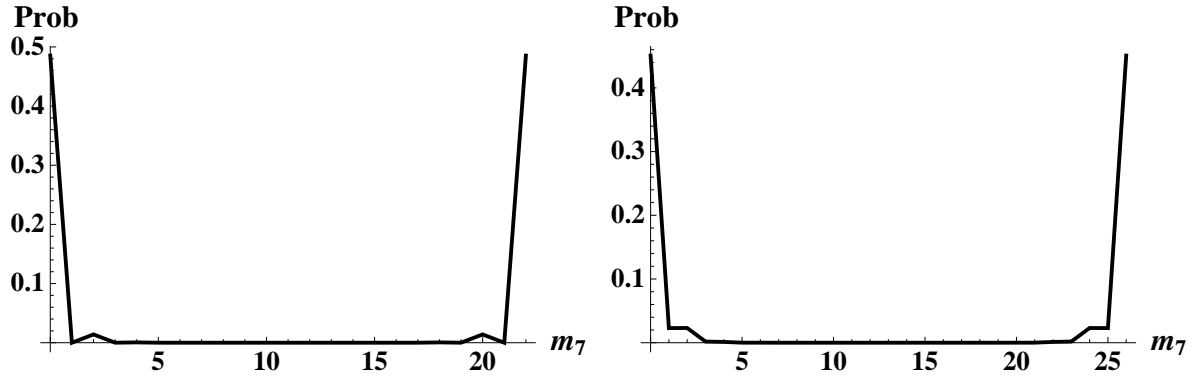


FIG. 5: $P_{m_1, m_2, m_7, m_8, m_9}$ versus m_7 when $\xi = -\pi/2$, $\zeta = \pi/2$ for: (Left) $N_\alpha = N_\beta = 35$, $m_1 = 22$, $m_2 = 8$, $m_9 = 18$ (the most probable value), $T = 0.37$, the value from Eq. (26). Here the NOON qualities are $q_1 = 0.97$ and $q_2 = 0.99$. (Right) Same parameters except with $m_9 = 14$. We find $q_1 = 0.91$ and $q_2 = 0.98$.

transmission is $T = 0.36$ and the average value of $\langle m_9 \rangle = 18.2$. When $m_9 = 14$, that is, a less probable value (the probability of getting this value relative to the most probable value is ~ 0.4), the distribution is only slightly less NOON-like.

There is a simple NOON quality factor to test the approximate NOON state, namely

$$q_1 = 2P_{m_1, m_2, 0, N-m_1-m_2-m_9, m_9} \quad (36)$$

that is, twice the value of the probability at $m_7 = 0$; we would like q_1 to be as close to 1.0 as possible. The NOON quality for the $m_9 = 18$ case in Fig. 5 is 0.97; for $m_9 = 14$ it is 0.91. Even when the probability of having $m_7 = 0$ or $m_7 = N - m_1 - m_2 - m_9$ is high, it is possible to imagine a peculiar situation where the rest of the particles might be situated near $m_7/2$, which would diminish the NOON quality of the state. A quality factor that takes this into account is

$$q_2 = 4 \frac{\Delta^2 m_7}{m_{78}^2} \quad (37)$$

where $\Delta^2 m_7 = \langle m_7^2 \rangle - \langle m_7 \rangle^2$ is the variance of m_7 over the distribution. In a perfect NOON state the variance is maximal and $q_2 = 1$. The worst possible case might be when $P(m_7 = \frac{m_{78}}{2} - 1) = P(m_7 = \frac{m_{78}}{2} + 1) = 0.5$ with all others zero; this case has $q_2 = 0$. A case in which all probabilities are equal has $q_2 = 0.33$. The second quality number seems less sensitive to changes in the resulting NOON states, but compare them in the case shown in Fig. 6. While the first quality factor vanishes, the second one is greater than zero because there is some NOON-like separation in the two peaks.

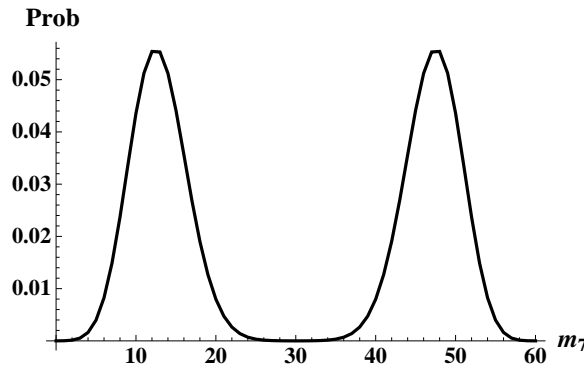


FIG. 6: Probability distribution for a poor quality attempted NOON. Here $N = 100$, $m_1 = 35$, $m_2 = 5$, $T = 1$ and $m_9 = 0$. The NOON quality factors are $q_1 = 0$ and $q_2 = 0.34$.

Next we choose a wide range of values of m_1 , m_2 to provide the thorough set of comparisons. The result given in Table I, which lists values of the optimal transmission coefficient at $N = 140$. The parameter

TABLE I: Quality factors for a wide range of input m_1 and m_2 values, with the resulting transmission coefficients and m_9 averages for $N = 140$.

m_1	m_2	m_{78}	$\langle m_9 \rangle$	T	q_1	q_2
45	5	18	72	0.11	0.976	0.990
40	10	36	54	0.25	0.968	0.993
35	15	54	36	0.43	0.955	0.993
30	20	72	19	0.67	0.932	0.992
25	25	90	0	1.0	0.883	0.988

$m_{78} = m_7 + m_8$ is the total number of particles involved in the NOON state. In each case the average value of m_9 is used.

It is likely, in any set of experimental runs, that a random assortment of values of m_1, m_2 , and m_9 will be averaged over in making a NOON state. What percentage of the inputs will result in good NOON states? In Appendix C we compare the corrected and uncorrected efficiencies and show that the correction process is successful in producing good quality NOON states with high probability.

VII. APPLICATIONS OF THE NOON STATE

A. Metrology

A key application of NOON states is to ultrasensitive sensors, with fundamental sources of noise reduced to the minimal level permitted by quantum mechanics [1, 16]. Fig. 7(i) shows a Mach-Zehnder interferometer set up for the measurement of a path-length difference χ , a model that can be applied to the detection of a variety of physical parameters. A wide variety of input states, measurement protocols, and decoherence models have been considered in the literature. In what follows, we will consider the usefulness of approximate NOON states generated by the interferometric method described previously. The phase estimation process can be considered as an additional interferometric stage at the output, as illustrated in Fig. 7(ii).

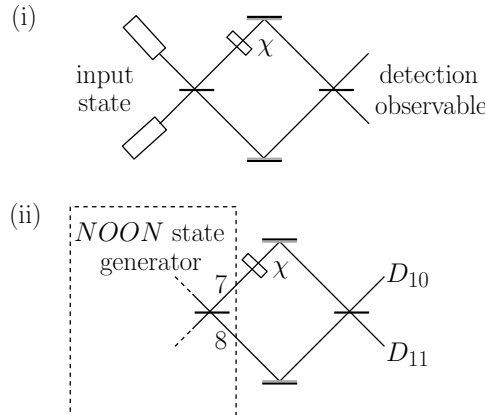


FIG. 7: The application of our NOON-state generator to phase estimation is illustrated. The aim is determine the unknown path-length difference in a Mach-Zehnder interferometer with precision approaching the Heisenberg limit. In (i), we show the usual Mach-Zehnder setup for measurement of phase. In (ii), an additional stage is added to the NOON generator for phase measurements. The NOON is in arms 7 and 8.

A typical phase estimation procedure is as follows. For each estimate of parameter χ , with value $\hat{\chi}$, the experiment is repeated t times. It is assumed that the (conditional) probability distributions $P(k|\chi)$, for the possible detection outcomes k , are known from theory. Following a Bayesian approach, the posterior distribution $P(\chi|k_t \cdots k_1)$ is obtained from the prior distribution $P(\chi)$ by the update rule $P(\chi|k_t \cdots k_1) \propto P(k_t|\chi) \cdots P(k_1|\chi) P(\chi)$. A suitable estimator - such as the mean value for $P(\chi|k_t \cdots k_1)$ - is applied to obtain a value for $\hat{\chi}$. For a so-called “global” estimation procedure no

prior information is assumed and $P(\chi) \propto 1/2\pi$; for a “local” estimation procedure, the aim is to track small changes of χ [17]. It is for the latter case that NOON states are particularly useful. A common measure of the statistical information available for a local estimation procedure is the (classical) Fisher information defined as $I_{\text{cl}} = \sum_k P(k|\chi) \left(\frac{d}{d\chi} \ln[P(k|\chi)] \right)^2$. Given a total of ν independent estimates $(\hat{\chi}_1, \dots, \hat{\chi}_\nu)$, the Cramer-Rao bound places a lower bound on precision $\Delta\chi$ (defined as the root mean-square error of the final estimate) as $\Delta\chi \geq 1/\sqrt{\nu I_{\text{cl}}}$. This bound may be assumed to be tight, provided ν is not too small, although we will not attempt to provide a detailed statistical analysis on this point.

Returning to the case of the phase-estimation procedure in Fig. 7(ii), I_{cl} is upper bounded by a value termed the quantum Fisher information I_{qu} . For the case of the interferometric detection of phase shifts using particle counting, I_{qu} can be straightforwardly derived (see Ref. 20, a special case of the analysis in Ref. 21), and for the interferometer in Fig. 7(ii) the value is $I_{\text{qu}} = 4\Delta^2 m_7$ (where $\Delta^2 m_7$ denotes the particle-number variance $\langle m_7^2 \rangle - \langle m_7 \rangle^2$). It is important to verify whether this bound is tight across the range of possible values for χ (many existing schemes are in fact suboptimal in this respect). To check this, we verify that the approximate NOON states at 7 and 8 satisfy the path-symmetry condition identified in Ref. 20. Applying the analysis to the amplitudes for positions 7 and 8, after m_1, m_2 and m_9 particles are counted at detectors D_1, D_2 , and D_9 ,

$$C_{m_1, m_2, m_7, m_8, m_9} \propto \langle 0 | \frac{a_1^{m_1} a_2^{m_2} a_7^{m_7} a_8^{m_8} a_9^{m_9}}{\sqrt{m_1! m_2! m_7! m_8! m_9!}} | N_\alpha N_\beta \rangle \quad (38)$$

the path-symmetry condition requires that,

$$C_{m_1, m_2, m_7, m_8, m_9} = (C_{m_1, m_2, m_8, m_7, m_9})^* e^{i\gamma} \quad (39)$$

where the phase factor $e^{i\gamma}$ is the same for all possible values for m_7 and $m_8 = N - M - m_7$ (where $M = m_1 + m_2 + m_9$ and $N = N_\alpha + N_\beta$), and indices 7 and 8 have been swapped. For the amplitudes $C_{m_1, m_2, m_7, m_8, m_9}$, this condition can be verified by inspecting the explicit forms of the operators a_i , given by Eq. (2), under (scalar) complex conjugation. As previously it is assumed that $(\theta = \pi/2, ie^{i\xi} = \pm 1$ and $\zeta = \pi/2)$. Since a_1, a_2 , and a_9 are proportional to $a_\alpha \pm a_\beta$, complex conjugation generates only a fixed phase factor contributing to γ in the path-symmetry condition. In addition we find $(a_8)^* = ia_7$ and $(a_7)^* = ia_8$. Hence complex conjugation swaps the 7 and 8 labels, and contributes a fixed factor of $(m_7 + m_8)\pi/2$ to γ .

To compare the usefulness for phase estimation of states with the same total particle number $m_7 + m_8$, we adopt the quality factor of Eq. (37) $q_2 = 4(\Delta^2 m_7)/(m_7 + m_8)^2$; q_2 is normalized between 0 and 1, with the maximum value being attained by a perfect NOON state. For the input state $|N_\alpha N_\beta\rangle$ combined at a beam splitter, with $N_\alpha = N_\beta = (m_7 + m_8)/2$ (assumed to be even), q_2 has the value $1/2 + 1/(m_7 + m_8)$. In particular, there is already a Heisenberg-limit type scaling for the precision, which at larger particle numbers is less than that for a corresponding NOON state by a constant factor of $\sqrt{2}$.

While the direct dual-Fock-state method has a smaller precision by $\sqrt{2}$ than the corrected NOON method, one must also consider how many particles the corrected device “loses” in the detectors D1, D2, and D9, especially if the total number of quantum sources N is limited. If the final output contains a fraction f of the original source number, $m_{78} = fN$, then to exceed the dual-Fock-state method in phase accuracy we require

$$\frac{1}{f\sqrt{q_2}} \leq \sqrt{2} \quad (40)$$

For $q_2 = 0.95$ we have $f \geq 0.72$. For, say, $N = 60$ that would require $m_{78} \geq 44$. We have repeated the averaging calculation shown in Fig. 9 for $m_{78} = 44$ and find in that case $q_1 = 0.81, q_2 = 0.96$ (still a very high value!). However the absolute probability of that particular value of m_{78} is only 6×10^{-6} compared to the value 0.02 for $m_{78} = 20$ of Fig. 9. Higher values of m_{78} become even less likely. Thus the direct dual-Fock-state process may well provide a more efficient use of limited source resources.

B. Probing the state

Here we consider the uncorrected case of Sec. III where we took $m_1 = m_2$ so the NOON is formed in arms 5 and 6 and interferes at the last beam splitter with detection in 7 and 8. We take $\zeta = 0$ we also

have $\theta = \pi/2$ and $\xi = 0$ (as above in Sec. III), in which case we find

$$P_{m_1, m_2, m_7, m_8} = \frac{K}{m_7! m_8!} \left| \sum_{p=0}^{m_1} \frac{(-1)^p}{p!(m_1 - p)!(N_\alpha - p - m_8)!(m_2 + m_8 - N_\alpha + p)!} \right|^2 \quad (41)$$

where K is a normalization factor. A plot of this probability versus m_7 is shown in Fig. 8. The oscillations are equivalent to interference fringes and are similar to those found in Ref. 22 where the phase states shown in Fig. 10 were allowed to interfere.

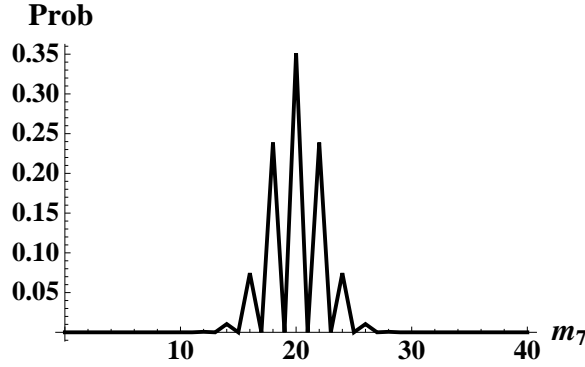


FIG. 8: Plot of P_{m_1, m_2, m_7, m_8} of Eq. (41) versus m_7 for $m_1 = m_2 = 40$, $N_\alpha = N_\beta = 40$. Here $\zeta = 0$. The solid line is the exact result; the dotted line is the approximation of Eq. (41).

The NOON superposition in the two arms is analogous to macroscopic particle interference in a two-slit experiment. As explained in more detail Ref. 15 any attempt to detect the arm in which the N particles travel results in the destruction of the interference pattern.

VIII. CONCLUSION

In conclusion, we have discussed a measurement-based approach to generating atomic NOON states with a high particle number, developing ideas first proposed in Refs. 14, 15. The key requirements for the method are dual-Fock state Bose-Einstein condensates for the input, atom interferometry, and particle counting, the basic experimental feasibility of which have already been demonstrated [24, 25]. In the photonic case both high-efficiency number-resolved detection [26] and feed-forward switching [27] have been demonstrated experimentally. However photon loss would make successful implementation of the scheme in a truly scalable manner very difficult [28]. We have shown using two different NOON quality factors that, when the number of detected particles is sufficiently high, the NOON states at the output are a very good approximation to the ideal. While dual-Fock states assumed for the input enable measurement precision better than the standard-quantum limit, and Heisenberg-limit-like scaling, NOON states saturate the Heisenberg limit, and represent the optimum strategy using nonclassical resources. One can also envisage macroscopic NOON states being used to demonstrate the quintessential two-slit experiment, in analogy to a large molecule propagating in a superposition state through a double slit, and re-interfering with itself at a screen.

In terms of the detailed analysis, the methodology differs somewhat from that used in Ref. 14. In contrast to the previous work, an integral representation of δ -functions is used (rather than working in an over-complete basis of coherent states). This approach is simpler; for example, the interferometer parameters can be determined by inspection of the binary form of the annihilation operators at various positions. We derive rigorously an algebraic condition for the transmission coefficient for the side-detections for the correction stage. The optimum value for the coefficient cannot be attained in practice, since it depends on the unknown outcome at the side detector itself. This problem is solved by substituting the mean particle count - the best strategy possible. A simple expression for the transmission coefficient is derived by considering the mean intensities in different arms of the interferometer. This leads to a new explanation of the feed-forward method, and the achievability of high values for the NOON quality factors.

Acknowledgements

H. C. acknowledges support for this work by the National Research Foundation and Ministry of Education, Singapore. Laboratoire Kastler Brossel is “UMR 8552 du CNRS, de l’ENS, et de l’Université Pierre et Marie Curie”.

Appendix A

We present here the derivation of Eqs. (32) and (33). We start with Eq. (28) and write

$$G_{m_a, m_b} = \frac{1}{4^N m_1! m_2!} \left| \langle 0 | (a_\alpha + a_\beta)^{m_1 + m_a} (a_\alpha - a_\beta)^{m_2 + m_b} | N_\alpha N_\beta \rangle \right|^2 \quad (42)$$

Then for fixed $m_{5'} + m_6 + m_9 = N - m_1 - m_2$ we have

$$\langle m_9 \rangle = \mathcal{N} \sum_{m_{5'}, m_6, m_9} \left[\delta_{m_{5'} + m_6 + m_9, M} m_9 \frac{T^{m_{5'}} R^{m_9}}{m_{5'}! m_6! m_9!} G_{m_{5'} + m_9, +m_6} \right] \quad (43)$$

where \mathcal{N} is a normalization constant. Change summation variables from $m_{5'}$ to $p = m_{5'} + m_9$. Then we can pull the G_{p, m_6} factor out of the sum on m_9 to get

$$\langle m_9 \rangle = \mathcal{N} \sum_{p, m_6} \left\{ \frac{\delta_{p+m_6, M}}{m_6! p!} G_{p+m_6} \sum_{m_9} \left[m_9 \frac{p! R^{m_9} T^{p-m_9}}{m_9! (p-m_9)!} \right] \right\} \quad (44)$$

Because $T + R = 1$ the sum on m_9 yields simply pR to give

$$\langle m_9 \rangle = \mathcal{N} R \sum_{m_6} \left\{ \frac{1}{m_6! (M - m_6)!} G_{p+m_6} (M - m_6) \right\} \quad (45)$$

An exactly analogous calculation leads to

$$\langle m_6 \rangle = \mathcal{N} \sum_{p, m_6} \left\{ \frac{\delta_{p+m_6, M}}{m_6! p!} m_6 G_{p+m_6} \sum_{m_9} \left[\frac{p! R^{m_9} T^{p-m_9}}{m_9! (M - m_9)!} \right] \right\} \quad (46)$$

The m_9 sum is just $(R + T)^p = 1$ so that

$$\langle m_6 \rangle = \mathcal{N} \sum_{m_6} \left\{ \frac{m_6}{m_6! (M - m_6)!} G_{p+m_6} \right\} \quad (47)$$

The resulting relation is

$$\langle m_9 \rangle = (1 - T) (N - m_1 - m_2 - \langle m_6 \rangle) \quad (48)$$

which is Eq. (29).

By particle conservation we have

$$\langle m_5 + m_6 \rangle = N - m_1 - m_2 \quad (49)$$

Note the prime is missing from the m_5 number here ($m_5 = m_{5'} + m_9$).

We can also prove a relation between $\langle m_5 \rangle$ and $\langle m_6 \rangle$. From Eq. (7), with appropriate values of the phase shifts entered, we have

$$\begin{aligned} P_{m_1, m_2, m_5, m_6} &= \frac{N_\alpha! N_\beta!}{4^N m_1! m_2! m_5! m_6!} \int_{-\pi}^{\pi} \frac{d\phi'}{2\pi} \int_{-\pi}^{\pi} \frac{d\phi}{2\pi} e^{-iN_\alpha(\phi - \phi')} \left[(e^{-i\phi'} + 1)(e^{i\phi} + 1) \right]^{m_1 + m_5} \\ &\quad \times \left[(e^{-i\phi'} - 1)(e^{i\phi} - 1) \right]^{m_2 + m_6} \end{aligned} \quad (50)$$

If we change variables to $\Lambda = (\phi - \phi')/2$ and $\lambda = (\phi + \phi')/2$ we find

$$P_{m_1, m_2, m_5, m_6} = \frac{N_\alpha! N_\beta!}{m_1! m_2! m_5! m_6! 2^N} \int_{-\pi}^{\pi} \frac{d\lambda}{2\pi} \int_{-\pi}^{\pi} \frac{d\Lambda}{2\pi} \cos[(N_\alpha - N_\beta) \Lambda] \times [\cos \Lambda + \cos \lambda]^{m_1+m_5} [\cos \Lambda - \cos \lambda]^{m_2+m_6} \quad (51)$$

To find $\langle m_5 \rangle$ multiply this by m_5 and sum over m_5 and m_6 subject to the restriction that $m_5 + m_6 = N - m_1 - m_2$; the sum is

$$S = \sum_{m_5, m_6} \frac{m_5}{m_5! m_6!} [\cos \Lambda + \cos \lambda]^{m_5} [\cos \Lambda - \cos \lambda]^{m_6} \frac{(\cos \Lambda + \cos \lambda)}{(N - m_1 - m_2 - 1)!} (2 \cos \Lambda)^{N - m_1 - m_2 - 1} \quad (52)$$

This results in the average

$$\langle m_5 \rangle = K_{m_1 m_2} (m_1 + 1) F(m_1 + 1, m_2) \quad (53)$$

where

$$F(m_1, m_2) = \frac{1}{m_1! m_2!} \int_{-\pi}^{\pi} \frac{d\lambda}{2\pi} \int_{-\pi}^{\pi} \frac{d\Lambda}{2\pi} \cos[(N_\alpha - N_\beta) \Lambda] \times (\cos \Lambda)^{N - m_1 - m_2} [\cos \Lambda + \cos \lambda]^{m_1} [\cos \Lambda - \cos \lambda]^{m_2} \quad (54)$$

and $K_{m_1 m_2}$ contains other factors unimportant for our purposes. A similar equation is found for $\langle m_6 \rangle$:

$$\langle m_6 \rangle = K_{m_1 m_2} (m_2 + 1) F(m_1, m_2 + 1) \quad (55)$$

For large $N - m_1 - m_2$ the $(\cos \Lambda)^{N - m_1 - m_2}$ factor peaks very sharply at $\Lambda = 0$ and can be replaced by $D_{m_1 m_2} \delta(\Lambda)$, where $D_{m_1 m_2}$ is a factor that can be lumped into $K_{m_1 m_2}$. The result is that

$$F(m_1, m_2) \cong \frac{1}{m_1! m_2!} \int_{-\pi}^{\pi} \frac{d\lambda}{2\pi} [1 + \cos \lambda]^{m_1} [1 - \cos \lambda]^{m_2} = \frac{1}{m_1! m_2!} \frac{2^{m_1+m_2+1} \Gamma(m_1 + \frac{1}{2}) \Gamma(m_2 + \frac{1}{2})}{(m_1 + m_2)!} \quad (56)$$

yielding the result

$$\frac{\langle m_5 \rangle}{\langle m_6 \rangle} \cong \frac{m_1 + \frac{1}{2}}{m_2 + \frac{1}{2}} \approx \frac{m_1}{m_2} \quad (57)$$

which is Eq. (31).

Appendix B

We want to find a rigorous formula for $\langle m_9 \rangle$. Starting from Eq. (28) we expand the operators, take matrix elements, yielding a δ -function, which we replace by an integral:

$$C_{m_1, m_2, m_5', m_6, m_9} = \frac{\sqrt{T^{m_5} R^{m_9} N_\alpha! N_\beta!}}{2^N \sqrt{m_1! m_2! m_5'! m_6! m_9!}} \times \int_{-\pi}^{\pi} \frac{d\phi}{2\pi} e^{-i N_\alpha \phi} (e^{i\phi} + 1)^{m_1+m_5'+m_9} (e^{i\phi} - 1)^{m_2+m_6} \quad (58)$$

$$= \frac{\sqrt{T^{m_5} R^{m_9} N_\alpha! N_\beta!}}{\sqrt{m_1! m_2! m_5'! m_6! m_9!}} \quad (59)$$

$$\times \int_{-\pi}^{\pi} \frac{d\phi}{2\pi} e^{-i(N_\alpha - N_\beta)\phi} \left(\cos \frac{\phi}{2} \right)^{m_1+m_5'+m_9} \left(\sin \frac{\phi}{2} \right)^{m_2+m_6} \quad (60)$$

If $N_\alpha = N_\beta$ the integral can be done analytically. We sum the result over all $m_{5'}$ and m_6 to give:

$$P_{m_1, m_2, m_9} = \frac{\mathcal{N} R^{m_9}}{m_9!} \sum_{m_{5'}=0}^{N-\mathcal{M}} \frac{T^{m_5}}{(m_{5'})!(N-\mathcal{M}-m_{5'})!} \{ [1 + (-1)^{m_2+N-\mathcal{M}-m_{5'}}] \times \Gamma\left(\frac{1+m_1+m_{5'}+m_9}{2}\right) \Gamma\left(\frac{1+m_2+N-\mathcal{M}-m_{5'}}{2}\right) \}^2 \quad (61)$$

where \mathcal{N} is a normalization factor.

Fig. 9 shows a plot of P_{m_1, m_2, m_9} of Eq. (61) for a set of variables having a large value of $\langle m_9 \rangle$. To get this plot we used $T = m_2/m_1$. We find the exact result $\langle m_9 \rangle = 53.6$ compared to the approximation of 54 given by Eq. (33).

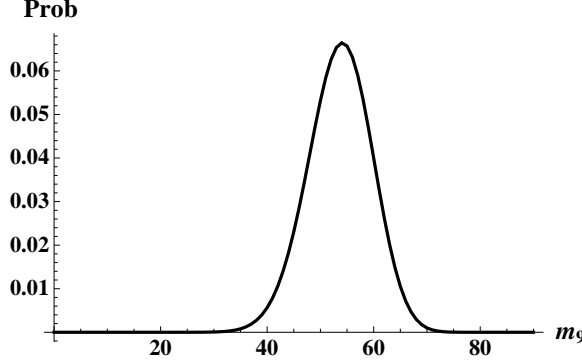


FIG. 9: P_{m_1, m_2, m_9} of Eq. (13) versus m_9 for $N_\alpha = N_\beta = 70$, $m_1 = 40$, $m_2 = 10$. We find $\langle m_9 \rangle = 53.6$, while the approximate formula of Eq. (33) gives 54.

Appendix C: Circuit Efficiency comparisons

It is likely, in any set of experimental runs, that a random assortment of values of m_1, m_2 , and m_9 will be averaged over in making a NOON state. What percentage of the inputs will result in good NOON states? Here we compare the corrected and uncorrected efficiencies to get an idea of how successful is the correction circuit in providing good NOON states.

A. Uncorrected Circuit

With the uncorrected circuit one can, for a given N value, compute in the 2D space of $\{m_1, m_2\}$, the various possible NOON output numbers, $m_{56} = N - m_1 - m_2$, and the corresponding NOON quality factor q_1 and total absolute probability (probability normalized over all five m variables) of getting each result. In a 2D plot of the probability one finds the highest q_1 factors along $m_1 = m_2$, as expected. This line of high q_1 is a minimum of absolute probability – nonequal m_1, m_2 values are more probable. A sample is shown in Fig. 10 for $N = 60$ and $m_{56} = 20$. Note that only the middle seven m_1 values give a quality factor greater than 0.90 and only the middle three are greater than 0.95. When m_{56} is larger, the quality factors drop so that for, say, $m_{56} = 30$ only the case $m_1 = m_2 = 15$ gives $q_1 = 0.95$ and only the middle three points have $q_1 > 0.90$. As m_{56} decreases, the distribution of high quality factors broadens greatly, but one is then getting fewer NOON particles as output, and the absolute probability of occurrence of these states is lower.

We can average the data of Fig. 10 over all m_1 to get a NOON that would occur if we accepted *all* events at constant $m_{56} = 20$. The result is shown in Fig. 11. The resulting quality factor is low (0.26) because we have averaged over some very poor states. The total probability of getting any results corresponding to $m_{56} = 20$ is 0.0036.

We can assume that someone using the uncorrected circuit would be more selective and keep only data associated with m_1 values that have higher quality factors and sufficiently large m_{56} values. Thus if one

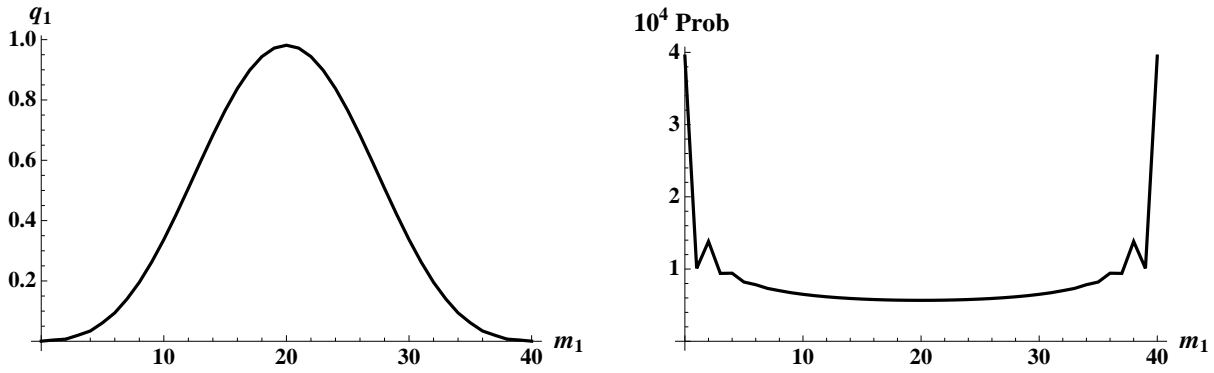


FIG. 10: Uncorrected circuit quality factor (left) and absolute probability (right) for fixed $N = 60$, $m_{56} = 20$ as a function of m_1 . The best quality occurs for $m_1 = m_2$. Note that the probability is smallest for the best quality factor.

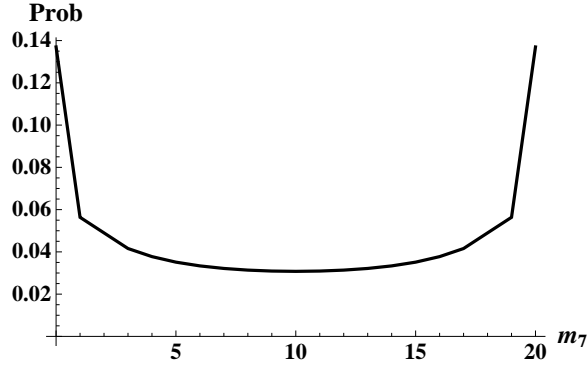


FIG. 11: The NOON state resulting from averaging over all m_1 corresponding to fixed $N = 60$, $m_{56} = 20$. The quality factors are low: $q_1 = 0.27$ and $q_2 = 0.53$.

demands that the NOON output particle number m_{56} be 20 or larger (still for $N = 60$) for $q_1 = 0.90$, one will get this 6.2% of the time. Table II shows the percentages for various output minimum numbers.

B. Corrected Circuit

In the corrected circuit we have one more variable m_9 , making it very difficult to get the data set equivalent to that which led to, say, Table II. However, we can analyze a particular case corresponding to fixed values of N and output number m_{78} . We again choose $N = 60$ and $m_{78} = 20$. First we present a NOON that is a probability-weighted average over all m_1, m_2 , and m_9 corresponding to those values. Of course, we have $m_9 = N - m_{78} - m_1 - m_2$ determined for each set of the variables m_1 and m_2 . Thus we

TABLE II: Probability $P_{N_{min}}$ (in percent) for getting a NOON with quality q_1 and output number greater or equal to N_{min} for $N = 60$ for an uncorrected circuit.

N_{min}	% ($q_1 = 0.90$)	% ($q_1 = 0.95$)
35	0.30	0
30	2.7	0.2
20	6.2	1.6
15	6.2	2.0

have a double sum with the probability distribution given by

$$P_{78} = \sum_{m_1=0}^{M/2} \left\{ P_{m_1, m_1, m_7, m_8, m_9} + 2 \sum_{m_2=m_1+1}^{M-m_1} P_{m_1, m_2, m_7, m_8, m_9} \right\} \quad (62)$$

where $M = N - m_{78}$ and the factor of 2 in the second term takes account of the symmetry that occurs when m_1 and m_2 are interchanged. The NOON state produced by this process is shown in Fig. 12. The efficiency in getting this high quality result ($q_1 = 0.94$) is good; that is, output corresponding to

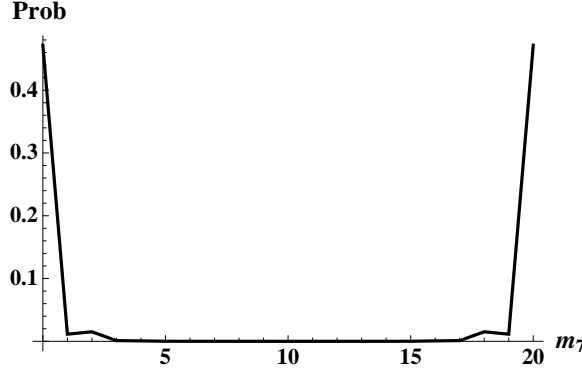


FIG. 12: The NOON state resulting from averaging over all m_1 and m_2 corresponding to fixed $N = 60$, $m_{78} = 20$. The q_1 quality factor is 0.94, while $q_2 = 0.98$

any element with this output number m_{78} occurs with absolute probability 2.1%. This NOON quality comes without any selection of specially chosen values of m_1 and m_2 as occurred in Table I. The point is that the m_9 probability distribution is small away from the high quality points because the transmission coefficient has been chosen properly.

We can see how the probability distribution selects high quality by taking apart the above NOON output. An important aspect of this is the position in $\{m_1, m_2\}$ space for which the actual value of $m_9 = N - m_{78} - m_1 - m_2$ is equal to its most likely value, given by Eq. (33). This is the position in the space where the absolute probability will be the largest. Moreover, we expect that the quality factor will be largest here too. Fig. 13 shows the plot of the points where this match of the real m_9 agrees with its most probable value. Suppose we now pick a value of m_1 and plot the quality factor and probability

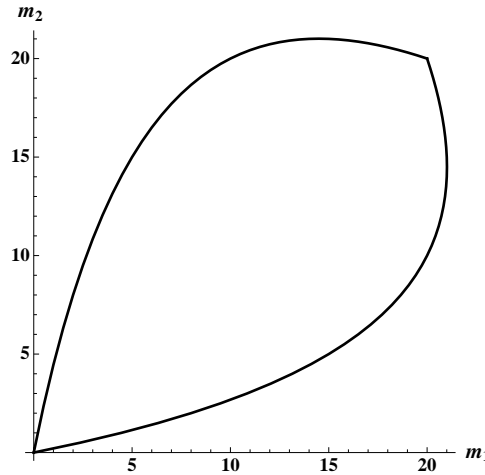


FIG. 13: Plot of the position in the $\{m_1, m_2\}$ grid at which m_9 matches its most probable value for $N = 60$ and $m_{78} = 20$.

versus m_2 : Fig. 14 shows these for $m_1 = 10$. There are two peaks in the quality factor corresponding to where m_2 crosses the places of maximum probability seen in Figure 13. The cusp occurs at the point

$m_1 = m_2 = 10$ where one switches from having $T = m_2/m_1$ to the inverse. The probability shows only the peak at the second crossing; there is also a peak at the first crossing, but it is too small to appear on the graph. Other samples of such plots show the probability similarly peaking at the point of largest

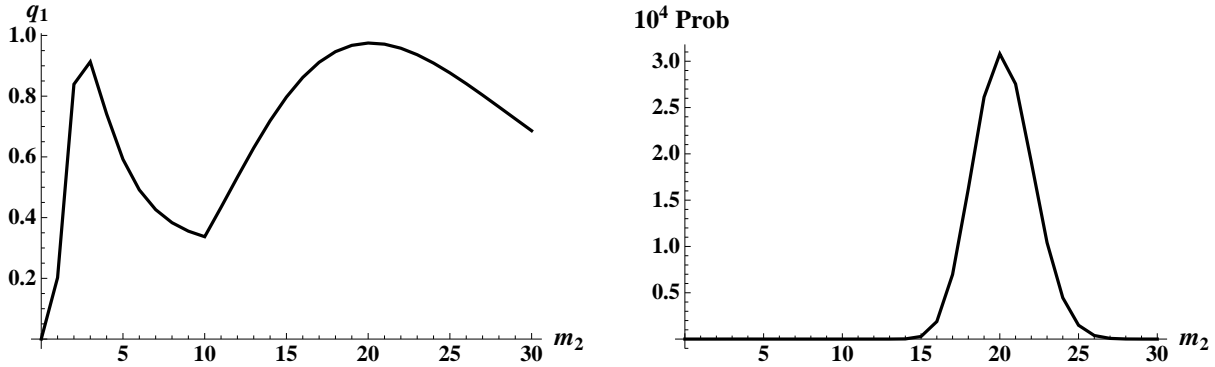


FIG. 14: Plots of the quality factor q_1 (left) and absolute probability (right) versus m_2 at fixed $m_1 = 10$ for $N = 60$, $m_{78} = 20$.

quality factor.

Finally we plot in Fig. 15 the quality factor and probability, *summed* over all m_2 , as a function of m_1 , again for fixed $N = 60$, $m_{78} = 20$. There are two peaks in the probability since, according to Fig. 13, there are equal probability regions in the $\{m_1, m_2\}$ space symmetrically at $\{10, 20\}$ and $\{20, 10\}$.

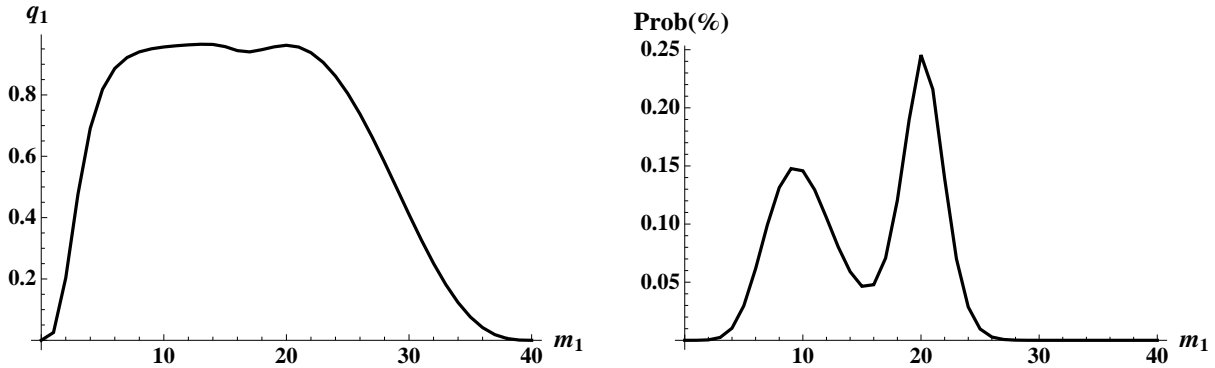


FIG. 15: Plots of the quality factor q_1 (left) and absolute probability (right), summed over all m_2 , versus m_1 at fixed $m_1 = 20$ for $N = 60$, $m_{78} = 20$.

Clearly the correction process is successful in producing good quality NOON states with high probability.

-
- [1] J. P. Dowling, Contemp. Phys. 49, 125 (2008).
 - [2] A. J. Leggett, Prog. Theor. Phys. Suppl. 69, 80 (1980); J. Phys. Condens. Matter 14, R415 (2002); Phys. Scr. T102, 69 (2002).
 - [3] D. M. Greenberger, M. A. Horne, A. Shimony, and A. Zeilinger, Am. J. Phys. 58, 1131 (1990).
 - [4] N. D. Mermin, Phys. Rev. Lett. 65, 1838 (1990).
 - [5] C. F. Wildfeuer, A. P. Lund, and J. P. Dowling, Phys. Rev. A 76, 052101 (2007).
 - [6] J. J. Bollinger, Wayne M. Itano, and D. J. Wineland, Phys. Rev. A 54, R4649 (1996); R. A. Campos, C. C. Gerry, and A. Benmoussa, Phys. Rev. A 68, 023810 (2003).

- [7] A. N. Boto, P. Kok, D. S. Abrams, S. L. Braunstein, C. P. Williams, and J. P. Dowling, *Phys. Rev. Lett.* 85, 2733 (2000); H. Cable, R. Vyas, S. Singh, and J. P. Dowling *New J. Phys.* 11, 113055 (2009).
- [8] M. W. Mitchell, J. S. Lundeen, and A. M. Steinberg, *Nature* 429, 161 (2004).
- [9] J. A. Jones, S. D. Karlen, J. Fitzsimons, A. Ardavan, S. C. Benjamin, G. Andrew, D. Briggs, and J. J. L. Morton, *Science* 324, 1166 (2009).
- [10] I. Afek, O. Ambar, Y. Silberberg, *Science* 328, 879 (2010).
- [11] P. Walther, J.-W. Pan, M. Aspelmeyer, R. Ursin, S. Gasparoni, and A. Zeilinger, *Nature* 429, 158 (2004).
- [12] T. Nagata, R. Okamoto, J. L. O'Brien, K. Sasaki, S. Takeuchi, *Science* 316, 726 (2007).
- [13] C. K. Hong, Z. Y. Ou, and L. Mandel, *Phys. Rev. Lett.* 59, 2044 (1987).
- [14] H. Cable and J. P. Dowling, *Phys. Rev. Lett.* 99, 163604 (2007).
- [15] W. J. Mullin and F. Laloë, *J. Low Temp. Phys.* 162, 250 (2011).
- [16] V. Giovannetti, S. Lloyd, L. Maccone, *arXiv:1102.2318v1*.
- [17] G. A. Durkin and J. P. Dowling, *Phys. Rev. Lett.* 99, 070801 (2007).
- [18] M. J. Holland and K. Burnett, *Phys. Rev. Lett.* 71, 1355 (1993).
- [19] S. L. Braunstein, C. M. Caves, and G. J. Milburn, *Ann. Phys.* 247, 135 (1996).
- [20] H. F. Hofmann, *Phys. Rev. A* 79, 033822 (2009).
- [21] G. A. Durkin, *New J. Phys.* 12, 023010 (2010).
- [22] W. J. Mullin and F. Laloë, *Phys. Rev. Lett.* 104, 150401 (2010).
- [23] A. J. Leggett and A. Garg, *Phys. Rev. Lett.* 54, 857 (1985).
- [24] Y.-J. Wang, D. Z. Anderson, V. M. Bright, E. A. Cornell, Q. Diot, T. Kishimoto, M. Prentiss, R. A. Saravanan, S. R. Segal, and S. Wu, *Phys. Rev. Lett.* 94, 090405 (2005).
- [25] W. S. Bakr, J. I. Gillen, A. Peng, S. Fölling, and M. Greiner, *Nature* 462, 74 (2009).
- [26] D. Rosenberg, A. E. Lita, A. J. Miller, and S. W. Nam, *Phys. Rev. A* 71, 061803(R) (2005)
- [27] R. Prevedel, P. Walther, F. Tiefenbacher, P. Böhi, Rainer Kaltenbaek, T. Jennewein, and A. Zeilinger, *Nature* 445, 65 (2007).
- [28] X. Chen and L. Jiang, J., *Phys. B At. Mol. Opt. Phys.* 40, 2799 (2007).